Diaminoanthracene Derivatives as High-Performance Green Host Electroluminescent Materials

Ming-Xin Yu,[†] Jiun-Pey Duan,[†] Chien-Hong Lin,[†] Chien-Hong Cheng,*[,†] and Yu-Tai Tao[‡]

Department of Chemistry, Tsing Hua University, Hsinchu, Taiwan 300, and Institute of Chemistry, Academia Sinica, Taipei, Taiwan 115

Received April 24, 2002. Revised Manuscript Received July 25, 2002

Diaminoanthracene derivatives 9,10-bis(1-naphthylphenylamino)anthracene (α-NPA), 9,10-bis(2-naphthylphenylamino)anthracene (*β*-NPA), 9,10-bis(*m*-tolylphenylamino)anthracene (TPA), and 9,10-bis(diphenylamino)anthracene (PPA) were conveniently synthesized from the corresponding diarylamine and 9,10-dibromoanthracene in the presence of $Pd(OAc)_2$, tri-*tert*-butylphosphine, and sodium *tert*-butoxide in *o*-xylene. Electroluminescent devices using α-NPA, *β*-NPA, and PPA as the hole transporters and host emitters were made. Devices consisting of diaminoanthracene (α-NPA, *β*-NPA, or PPA)/Alq_3 were shown to emit intensive green light from the diaminoanthracene layer instead of the Alq_3 layer. The device performance can be further improved by employing CuPc as the hole-injection layer, α-NPB or *m*-MTDATA as the hole-transporting layer, and Alq_3 or TPBI as the electron-transporting layer. Very high brightness, current, and power efficiencies and excellent CIE coordinates can be achieved by a suitable combination of these layers. For example, device **K**, which consists of *m*-MTDATA(20 nm)/*β*-NPA(40 nm)/TPBI(50 nm), emits green light at 530 nm and shows a maximum external quantum efficiency of 3.68%, current efficiency of 14.79 cd/A, power efficiency of 7.76 lm/W, and maximum brightness of 64991 cd/m^2.

Introduction

Since the groundwork by Tang and co-workers,[1] OLED has continued to be a subject of great interest to researchers in various fields due to its potential application in flat panel displays. The search for efficient and stable new emitting materials with proper CIE values for full-color displays remains as one of the most active areas of these studies. Among the well-known light-emitting materials, Alq_3 is considered as the most commonly used green host emitter. The Alq_3-based devices have been investigated in detail and have shown excellent properties in fabrication, lifetime, and brightness.[2−13] In addition to Alq_3 and its derivatives,[14,15] many green-light emitters have appeared in the literature.[16−26] $BeBq_2$ is known as an effective green-light host emitter.[16] Several carbazole derivatives have recently shown to be very efficient both as hole transporters and green emitters.[23] Devices employing dopant emitters such as coumarins[2,13] and quinacridones[6,7] in Alq_3 layers have achieved very high luminance. However, these dopant materials are not suitable for use as host emitters due to severe self-quenching. Recently, organic light-emitting diodes based on iridium com-

* To whom correspondence should be addressed.
[†] Tsing Hua University.
[‡] Academia Sinica.

(1) Tang, C. W.; Van Slyke, S. A. *Appl. Phys. Lett.* **1987**, *51*, 913.
(2) Tang, C. W.; Van Slyke, S. A.; Chen, C. H. *J. Appl. Phys.* **1989,** *65*, 3610.
(3) Shirota, Y.; Kuwabara, Y.; Inada, H.; Wakimoto, T.; Nakada, H.; Yonemoto, Y.; Kawami, S.; Imai, K. *Appl. Phys. Lett.* **1994**, *65*, 807.
(4) Tang, C. W.; Van Slyke, S. A.; Chen, C. H. *Appl. Phys. Lett.* **1996**, *69*, 2160.
(5) Tokito, S.; Tanaka, H.; Okada, A.; Taga, Y. *Appl. Phys. Lett.* **1996**, *69*, 878.
(6) Shi, J.; Tang, C. W. *Appl. Phys. Lett.* **1997**, *70*, 1665.
(7) Jabbour, G. E.; Kawabe, Y.; Shaheen, S. E.; Wang, J. F.; Morrell, M. M.; Kippelen, B.; Peyghambarian, N. *Appl. Phys. Lett.* **1997**, *71*, 1762.
(8) Jabbour, G. E.; Kippelen, B.; Armstrong, N. R.; Peyghambarian, N. *Appl. Phys. Lett.* **1998**, *73*, 1185.
(9) Kido, J.; Matsumoto, T. *Appl. Phys. Lett.* **1998**, *73*, 2866.
(10) Matsumura, M.; Furukawa, K.; Jinde, Y. *Thin Solid Films* **1998**, *331*, 96.
(11) Deng, Z. B.; Ding, X. M.; Lee, S. T.; Gambling, W. A. *Appl. Phys. Lett.* **1999**, *74*, 2227.
(12) Uekawa, M.; Miyamoto, Y.; Ikeda, H.; Kaifu, K.; Ichi, T.; Nakaya, T. *Thin Solid Films* **1999**, *352*, 185.
(13) Chen, C. H.; Tang, C. W. *Appl. Phys. Lett.* **2001**, *79*, 3711.
(14) Kido, J.; Iizumi, Y. *Chem. Lett.* **1997**, 963.
(15) Sapochak, L. S.; Padmaperuma, A.; Washton, N.; Endrino, F.; Schmett, G. T.; Marshall, J.; Fogarty, D.; Burrows, P. E.; Forrest, S. R. *J. Am. Chem. Soc.* **2001**, *123*, 6300.
(16) Hamada, Y.; Sano, T.; Fujita, M.; Fujii, T.; Nishio, Y.; Shibata, K. *Chem. Lett.* **1993**, 905.
(17) Chen, C. H.; Shi, J. *Coord. Chem. Rev.* **1998**, *171*, 161.
(18) Hamada, Y.; Kanno, H.; Sano, T.; Fujii, H.; Nishio, Y.; Takahashi, H.; Usuki, T.; Shibata, K. *Appl. Phys. Lett.* **1998**, *72*, 1939.
(19) Okada, K.; Wang, Y. F.; Chen, T. M.; Nakaya, T. *Thin Solid Films* **1999**, *346*, 69.
(20) Baldo, M. A.; Lamansky, S.; Burrows, P. E.; Thompson, M. E.; Forrest, S. R. *Appl. Phys. Lett.* **1999**, *75*, 4.
(21) Adachi, C.; Baldo, M. A.; Forrest, S. R.; Thompson, M. K. *Appl. Phys. Lett.* **2000**, *77*, 904.
(22) Lamansky, S.; Djurovich, P.; Murphy, D.; Abdel-Razzaq, F.; Lee, H. E.; Adachi, C.; Burrows, P. E.; Forrest, S. R.; Thompson, M. E. *J. Am. Chem. Soc.* **2001**, *123*, 4304.
(23) Thomas, K. R. J.; Lin, J. T.; Tao, Y. T.; Ko, C. W. *J. Am. Chem. Soc.* **2001**, *123*, 9404.
(24) Mi, B. X.; Gao, Z. Q.; Lee, C. S.; Kwong, H. L.; Wang, N. B.; Lee, S. T. *J. Mater. Chem.* **2001**, *11*, 2244.
(25) Xie, H. Z.; Liu, M. W.; Wang, O. Y.; Zhang, X. H.; Lee, C. S.; Hung, L. S.; Lee, S. T.; Teng, P. F.; Kwong, H. L.; Zheng, H.; Che, C. M. *Adv. Mater.* **2001**, *13*, 1245.
(26) Su, Y. Z.; Lin, J. T.; Tao, Y. T.; Ko, C. W.; Lin, S. C.; Sun, S. S. *Chem. Mater.* **2002**, *14*, 1884.

10.1021/cm020414m CCC: $22.00
Published on Web 09/16/2002

plexes as dopant emitters were found to emit green light via a phosphorescent pathway giving extremely high brightness as well as current and power efficiencies.[20−22,25]

A series of diaminoanthracene derivatives also have been used as green host emitters in a patent,[27] but there is still no detailed data for electroluminescent devices based on these compounds as the host emitters. In this paper, we wish to report that by a proper choice of the hole-injection, hole-transporting, and electron-transporting materials, diaminoanthracene-derivative-based electroluminescent devices show high brightness and current efficiency, very narrow emission bandwidth, and excellent CIE coordinates. The physical data of these compounds and the performance of these devices are reported. Furthermore, a new effective method for the synthesis of these diamino compounds different from that reported previously is described.[27]

Experimental Section

General Information. All reactions were carried out under a nitrogen atmosphere in sealed reaction vessels and were heated in an oil bath. *o*-Xylene was dried from potassium hydroxide. palladium(II) acetate, tri-*tert*-butylphosphine (Strem Chemical), sodium *tert*-butoxide (Acros), 9,10-dibromoanthracene, diphenylamine, *N*-phenyl-1-naphthylamine, and *N*-phenyl-2-naphthylamine (Lancaster) were used as purchased. Melting points were measured on a Fargo MP-2D melting point apparatus and were uncorrected. ^{1}H NMR and ^{13}C NMR spectra were recorded with a Varian Mercury 400 or Unity Inova 500 spectrometers. Mass spectra were obtained on a JEOL JMS-SX102A HRGC/LC/MS instrument operating in EI mode at 70 eV. UV−vis spectra were recorded on a Hitachi U-3300 model while photoluminescence (PL) spectra were taken using a Hitachi F-4500 fluorescence spectrophotometer. The glass transition temperatures of compounds were determined by differential scanning calorimetry (DSC) under a helium atmosphere using a Seiko SII-EXSTAR 6000-DSC-6200 instrument.

OLED Fabrication and Measurement. The OLEDs were fabricated by vacuum deposition of the materials at 10^{-6} Torr onto a clean glass precoated with a layer of indium tin oxide with a sheet resistance of 25 Ω/square. The deposition rate for organic compounds and CuPc (copper phthalocyanine) is 1−2 Å s^{-1}. The cathode consisting of Mg:Ag alloy (10:1, 55 nm) was deposited by coevaporation of Mg and Ag metals with deposition rates of 5−7 and 0.5−0.7 Å s^{-1}, respectively. The cathode was then capped with Ag metal (100 nm) by evaporation of Ag with a rate of 3 Å s^{-1}. The electron-transporting materials are Alq_3 (tris[8-hydroxyquinoline]aluminum) or TPBI (1,3,5-tris[*N*-phenylbenzimidazol-2-yl]benzene), while the hole-transporting materials are NPB (4,4′-bis[1-naphthylphenylamino]biphenyl), *m*-MTDATA (4,4′,4″-tris[3-methylphenylamino]triphenylamine), or diaminoanthracene derivatives. The thicknesses of CuPc, hole-transporting, emitting, and electron-transporting layers are 10, 20, 40, and 50 nm, respectively. The effective area of the emitting diode is 9.00 mm^2. Current, voltage, and light intensity measurements were made simultaneously using a Keithley 2400 source meter and a Newport 1835-C optical meter equipped with a Newport 818-ST silicon photodiode. Electroluminescent (EL) spectra were measured on a Hitachi F-4500 fluorescence spectrophotometer. Photoelectron spectra were obtained on a Riken Keiki photoelectronic AC-2 spectrometer. All chemicals used for electroluminescent devices were further purified by vacuum sublimation.

General Procedure for the Synthesis of Diaminoanthracene Derivatives. To a 25-mL sidearm flask in a dry nitrogen box were added 9,10-dibromoanthracene (1.25 mmol), diarylamine (2.50 mmol), $Pd(OAc)_2$ (0.025 mmol, Pd/Br = 1%), tri-*tert*-butylphosphine (0.03 mmol), and sodium *tert*-butoxide (3.0 mmol). The flask was sealed with a septum and was then moved out of the nitrogen box. To the flask was injected via a syringe *o*-xylene (10 mL). The reaction mixture was heated and stirred at 120 °C under nitrogen for an appropriate time (10−16 h). The reaction mixture was then cooled to room temperature, filtered through a Celite and silica gel pad, and washed with dichloromethane. The filtrate was washed with water and then dried with $MgSO_4$. Concentration of the filtrate on a rotary evaporator followed by washing of the solid material with methanol afforded the desired crude product. The crude product was then dried at 120 °C in a vacuum and was purified further by sublimation at 4−6 × 10^{-3} Pa. Four compounds were synthesized from 9,10-dibromoanthracene and the corresponding amine according to this procedure. The yields and important spectral data are listed below.

9,10-Bis(1-naphthylphenylamino)anthracene (α-NPA). Yield: 62%. mp = 373 °C. ^{1}H NMR ($CDCl_3$, δ): 6.64 (q, J = 8.0 Hz, J = 7.5 Hz, 4 H), 6.77−6.83 (m, 2 H), 7.03−7.11 (m, 5 H), 7.15−7.28 (m, 6 H), 7.45−7.53 (m, 5 H), 7.67 (q, J = 8.0 Hz, 2 H), 7.91 (t, J = 7.0 Hz, J = 8.0 Hz, 2 H), 8.21 (d, J = 8.5 Hz, 2 H), 8.25−8.28 (m, 4 H). ^{13}C NMR ($CDCl_3$, δ): 118.44 (CH), 118.51 (CH), 119.86 (CH), 119.90 (CH), 122.93 (CH), 125.10 (CH), 125.21 (CH), 125.50 (CH), 125.73 (CH), 126.14 (CH), 126.52 (CH), 128.13 (C), 129.07 (CH), 131.90 (C), 135.28 (C), 139.29 (C), 142.71 (C), 150.61 (C). HRMS (*m*/*z*): calcd for $C_{46}H_{32}N_2$ 612.2565, found 612.2562.

9,10-Bis(*m*-tolylphenylamino)anthracene (TPA). Yield: 74%. mp = 248 °C. ^{1}H NMR ($CDCl_3$, δ): 2.21 (s, 6 H), 6.71 (d, J = 7.6 Hz, 2 H), 6.80−6.90 (m, 4 H), 6.99 (d, J = 11.6 Hz, 2 H), 7.03−7.09 (m, 6 H), 7.14 (t, J = 8.8 Hz, J = 6.8 Hz, 4 H), 7.31−7.35 (m, 4 H), 8.15−8.19 (m, 4 H). ^{13}C NMR ($CDCl_3$, δ): 21.64 (CH_3), 117.71 (CH), 120.32 (CH), 120.78 (CH), 121.10 (CH), 122.32 (CH), 125.08 (CH), 126.67 (CH), 129.06 (CH), 129.19 (CH), 131.85 (C), 137.40 (C), 138.97 (C), 147.68 (C), 147.86 (C). HRMS (*m*/*z*): calcd for $C_{40}H_{32}N_2$ 540.2565, found 540.2560.

9,10-Bis(diphenylamino)anthracene (PPA). Yield: 72%. mp = 368 °C. ^{1}H NMR ($CDCl_3$, δ): 6.87−6.90 (m, 4 H), 7.08−7.10 (m, 8 H), 7.15−7.20 (m, 8 H), 7.33 (q, J = 3.2 Hz, 4 H), 8.16 (q, J = 3.2 Hz, 4 H). ^{13}C NMR ($CDCl_3$, δ): 120.27 (CH), 121.30 (CH), 125.04 (CH), 126.75 (CH), 129.26 (CH), 131.81 (C), 137.37 (C), 147.68 (C). HRMS (*m*/*z*): calcd for $C_{38}H_{28}N_2$ 512.2252, found 512.2278.

9,10-Bis(2-naphthylphenylamino)anthracene (β-NPA). Yield: 72%. mp = 332 °C. ^{1}H NMR ($CDCl_3$, δ): 6.96 (q, J = 6.4 Hz, 2 H), 7.16−7.44 (m, 20 H), 7.51 (q, J = 4.4 Hz, 2 H), 7.70 (q, J = 6.8 Hz, J = 8.0 Hz, 4 H), 8.24−8.27 (m, 4 H). ^{13}C NMR ($CDCl_3$, δ): 115.95 (CH), 120.56 (CH), 121.34 (CH), 121.64 (CH), 123.95 (CH), 125.05 (CH), 126.32 (CH), 126.88 (CH), 127.24 (CH), 127.54 (CH), 129.04 (CH), 129.36 (CH), 131.84 (C), 134.14 (C), 134.47 (C), 137.45 (C), 145.50 (C), 147.71 (C). HRMS (*m*/*z*): calcd for $C_{46}H_{32}N_2$ 612.2565, found 612.2571.

Results and Discussion

α-NPA (Chart 1) was successfully prepared from 9,10-dibromoanthracene and *N*-phenyl-1-naphthylamine in *o*-xylene in the presence of $Pd(OAc)_2$/P(*t*-Bu)$_3$/NaO-*t*-Bu at 120 °C.[28] The palladium catalyst is very effective, giving the corresponding diamino product in good yields with only a low amount of the palladium catalyst (1%) used. A previous method using copper powder as the catalyst for the reaction of 9,10-diiodoanthracene and *N*-phenyl-1-naphthylamine requires a much higher reaction temperature and longer reaction time.[27] This new compound was characterized by ^{1}H and ^{13}C NMR

(27) Enokida, T.; Tamano, M.; Okutsu, S. European Patent 0 765 106 A2, 1997.

(28) Yamamoto, T.; Nishiyama, M.; Koie, Y. *Tetrahedron Lett.* **1998**, *39*, 2367.

Table 1. Physical Properties of Diaminoanthracene Derivatives

compound	$T_m/T_g/T_c$[a] (°C)	λ_{max}(abs)[b] (nm)	λ_{em}[b] (nm)	λ_{em}[c] (nm)	Q.Y.[d]	HOMO/LUMO (eV)
α-NPA	373/166/227	253, 349, 456	524	522	0.46	5.54/3.11
β-NPA	332/138/223	254, 316, 355, 463	536	526	0.61	5.54/3.11
TPA	248/103/169	253, 291, 456	526	518	0.83	5.51/3.05
PPA	368/na/na	252, 291, 453	524	516	0.79	5.64/3.18

[a] Obtained from DSC measurement; na = not detected. [b] Measured in a CH_2Cl_2 solution. [c] Measured in the solid state. [d] Measured in a CH_2Cl_2 solution by using fluoresein as a reference.

Chart 1

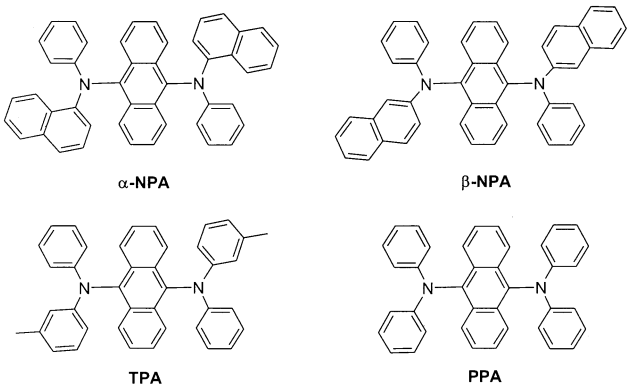

and mass spectral data. The proposed structure of this product is strongly supported by the number of signals in the NMR spectra. A total of 18 ^{13}C NMR signals were observed in agreement with the proposed symmetric nature of the structure. Three other diaminoanthracene derivatives (*β*-NPA, TPA, and PPA) were also synthesized smoothly from 9,10-dibromoanthracene and the corresponding diarylamine in good yields (Chart 1).

The physical data of these four diaminoanthracene derivatives α-NPA, *β*-NPA, TPA, and PPA synthesized are summarized in Table 1. Except TPA, all of these diamine species show melting points higher than 300 °C. Three of these compounds α-NPA, *β*-NPA, and TPA exhibit clear glass transition points (T_g) at 166, 138, and 103 °C, respectively, but there is no T_g observed for PPA. The observed glass transition points for α-NPA and *β*-NPA are much higher than those for NPB and *m*-MTDATA, which are comparable in molecular weight and are frequently used as hole transporters in organic light-emitting devices.[29,30] It is interesting to note that the T_g of α-NPA is close to that of the well-known EL material Alq_3.[15]

Figure 1 shows the UV−vis absorption in dichloromethane and photoluminescent spectra in the solid state of these diaminoanthracene derivatives. The lowest absorption maximum for these compounds all appear in the narrow region 453−463 nm with the wavelength in the order PPA < α-NPA ≈ TPA < *β*-NPA (Table 1). All these species emit light strongly both in solution and in the solid state. The quantum yields of these compounds in CH_2Cl_2 solution have been measured and are summarized in Table 1.[31] A narrow half-bandwidth (~65 nm) was observed for the PL spectrum of each compound except PPA, which shows a long tail in the 600-nm region (Figure 1). The emission maximums of these compounds fall in the range 516−526 nm with PPA giving the shortest emission peak at 516 nm (Table 1).

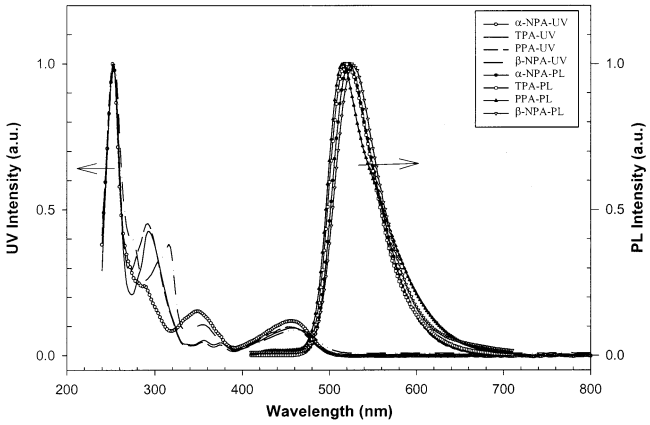

Figure 1. UV−vis absorption spectra in dichloromethane solutions and photoluminescent spectra in the solid state of the diaminoanthracene derivatives.

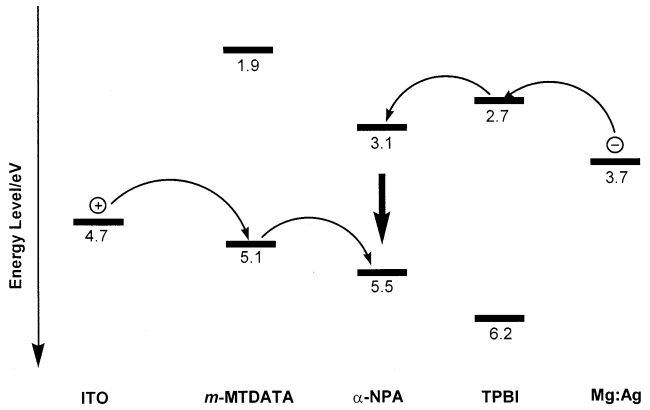

Figure 2. Relative HOMO/LUMO energy levels of device **F** (ITO/*m*-MTDATA/α-NPA/TPBI).

The HOMO and LUMO of these anthracene derivatives are also listed in Table 1. The HOMO was determined using a photoelectron spectrometer, while LUMO was calculated based on the HOMO energy level and the lowest-energy absorption edge of the UV−vis absorption spectrum.[32] The HOMO and LUMO energy of these products are at ca. 5.5−5.6 and 3.1−3.2 eV, respectively.

The observed strong emission at 522 nm in the solid state and high T_g point for α-NPA suggests that this diamine is potentially a green host emitter in organic electroluminescent devices. Several devices (**A**−**H**) were fabricated, aiming at understanding the emitting wavelength, emitting power, and the ability as a hole-transporting material of α-NPA. The relative energy levels of the materials used in one of these devices are displayed in Figure 2. Device **A** is a two-layer device consisting of the following layers: ITO/α-NPA(40 nm)/

(29) Koene, B. E.; Loy, D. E.; Thompson, M. E. *Chem. Mater.* **1998**, *10*, 2235.
(30) Shirota, Y.; Kobata, T.; Noma, N. *Chem. Lett.* **1989**, 1145.
(31) Brannon, J. H.; Magde, D. *J. Phys. Chem.* **1978**, *82*, 705.
(32) Janietz, S.; Bradley, D. D. C.; Grell, M.; Giebeler, C.; Inbasekaran, M.; Woo, E. P. *Appl. Phys. Lett.* **1998**, *73*, 2453.

Table 2. Performance of α-NPA-Based OLEDs[a]

device[b]	turn-on voltage (V)	external quantum efficiency (%, V)	brightness (cd/m^2, V)	current efficiency (cd/A, V)	power efficiency (lm/W, V)	CIE (x, y)	λ_{max} (nm)	fwhm (nm)
A	2.6	1.83, 7.0 (1.81, 7.4)	42056, 11.5 (6837)	6.93, 7.0 (6.84)	3.85, 5.5 (2.91)	0.24, 0.66	518	52
B	3.0	1.42, 6.0 (1.20. 8.2)	28634, 14.0 (4641)	5.51, 6.0 (4.66)	2.93, 5.5 (1.79)	0.23, 0.68	520	52
C	3.0	1.52, 8.5 (1.51, 8.1)	26522, 12.5 (4728)	4.74, 8.5 (4.73)	2.61, 5.0 (1.85)	0.22, 0.54	508	82
D	3.0	1.92, 4.5 (1.78, 5.4)	38534, 12.0 (6712)	7.28, 4.5 (6.72)	5.43, 4.0 (3.89)	0.23, 0.68	520	54
E	4.9	3.12, 9.5 (2.68, 12.2)	43364, 16.5 (10212)	11.92, 9.5 (10.24)	4.02, 9.0 (2.64)	0.24, 0.67	522	58
F	4.6	3.07, 7.5 (2.86, 8.3)	65129, 13.5 (11159)	12.05, 7.5 (11.23)	5.12, 7.0 (4.25)	0.24, 0.69	522	52
G	4.0	1.59, 6.5 (1.50, 7.3)	29500, 14.0 (5543)	5.88, 6.5 (5.55)	3.06, 6.0 (2.34)	0.18, 0.71	520	42
H	4.4	2.60, 7.0 (2.50, 7.4)	59844, 12.5 (9317)	9.74, 7.0 (9.37)	4.68, 6.5 (4.01)	0.20, 0.70	518	46

[a] The data for external quantum efficiency, brightness, current efficiency, and power efficiency are the maximum values of the device, and those in the parentheses were taken at a current density of 100 mA/cm^2. [b] Device **A**, α-NPA(40 nm)/Alq_3(50 nm); **B**, α-NPA(40 nm)/TPBI(50 nm); **C**, NPB(40 nm)/Alq_3(50 nm); **D**, NPB(20 nm)/α-NPA(40 nm)/TPBI(50 nm); **E**, *m*-MTDATA(20 nm)/α-NPA(40 nm)/Alq_3(50 nm); **F**, *m*-MTDATA(20 nm)/α-NPA(40 nm)/TPBI(50 nm); **G**, CuPc(10 nm)/NPB(20 nm)/α-NPA(40 nm)/TPBI(50 nm); **H**, CuPc(10 nm)/*m*-MTDATA(20 nm)/α-NPA(40 nm)/TPBI(50 nm).

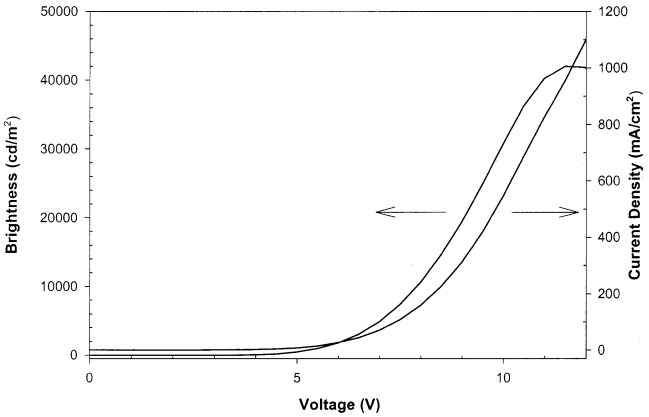

Figure 3. Luminance and current density versus voltage characteristics of device **A** (α-NPA/Alq_3).

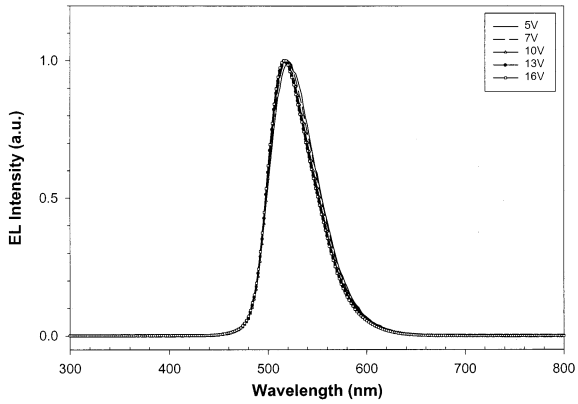

Figure 4. Electroluminescent spectra of device A (α-NPA/Alq_3) at various applied voltages.

Alq_3(50 nm). The luminance and current density versus voltage characteristics of this device are shown in Figure 3 and the EL spectra at various applied voltages are revealed in Figure 4. The device emits sharp green light at 518 nm with a fwhm of 52 nm as uncovered in Figure 4. Key electroluminescent data extracted from Figure 3 are listed in Table 2. A very low turn-on voltage (brightness = 1 cd/m^2) of 2.6 V with maximum brightness of 42056 cd/m^2 at 11.5 V, maximum external quantum efficiency of 1.83% at 7.0 V, and maximum power efficiency of 3.85 lm/W at 5.5 V, respectively, are achieved for this device. For comparison with other devices, electroluminescent data including external quantum efficiency, brightness, current, and power efficiency at 100 mA/cm^2 are also reported in the parentheses in the same table. The CIE coordinates calculated based on the EL data are (0.24, 0.66) (Figure 5). There is essentially no change in the EL spectrum (Figure 4) and CIE values between 5 and 16 V. The EL spectrum of device **A** closely resembles the PL spectrum of α-NPA, particularly in the half-bandwidth and the lowest and highest emission edges of the spectrum (Figures 1 and 4). Although Alq_3 also reveals a maximum emission at the wavelength very close to the value of **A**, its PL and EL spectra have much broader

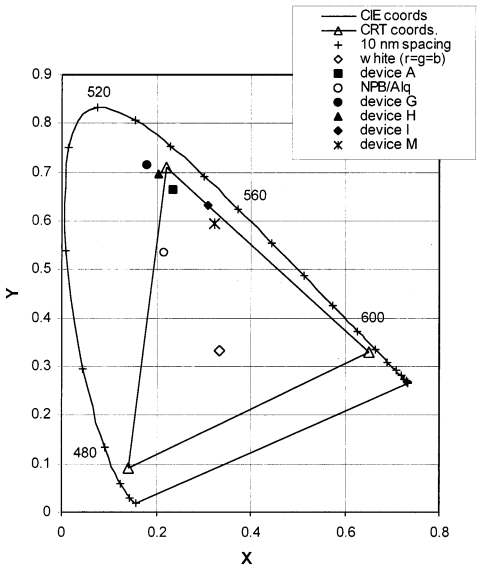

Figure 5. The Commission Internationale de L'Eclairage (CIE) chromaticity coordinates of devices **A** (α-NPA/Alq_3), **C** (NPB/Alq_3), **G** (CuPc/NPB/α-NPA/TPBI), **H** (CuPc/*m*-MTDATA/α-NPA/TPBI), **I** (β-NPA/Alq_3), and **M** (PPA/Alq_3).

Table 3. Performance of β-NPA-Based OLEDs[a]

device[b]	turn-on voltage (V)	external quantum efficiency (%, V)	brightness (cd/m^2, V)	current efficiency (cd/A, V)	power efficiency (lm/W, V)	CIE (x, y)	λ_{max} (nm)	fwhm (nm)
I	2.6	1.96, 6.0 (1.86, 7.6)	36863, 11.5 (7265)	7.69, 6.0 (7.27)	5.39, 4.0 (3.02)	0.31, 0.63	530	60
J	4.0	2.49, 8.5 (2.23, 10.2)	41488, 14.5 (8768)	9.81, 8.5 (8.78)	3.84, 8.0 (2.72)	0.32, 0.64	528	62
K	3.7	3.68, 6.0 (2.97, 8.5)	64991, 13.0 (11928)	14.79, 6.0 (11.94)	7.76, 6.0 (4.43)	0.33, 0.63	530	60
L	3.2	1.68, 7.5 (1.67, 7.6)	39701, 12.5 (6796)	6.80, 7.5 (6.80)	3.16, 6.0 (2.83)	0.31, 0.65	528	56

[a] The data for external quantum efficiency, brightness, current efficiency, and power efficiency are the maximum values of the device, and those in the parentheses were taken at a current density of 100 mA/cm^2. [b] Device **I**, β-NPA(40 nm)/Alq_3(50 nm); **J**, *m*-MTDATA(20 nm)/β-NPA(40 nm)/Alq_3(50 nm); **K**, *m*-MTDATA(20 nm)/β-NPA(40 nm)/TPBI(50 nm); **L**, NPB(20 nm)/β-NPA(40 nm)/TPBI(50 nm).

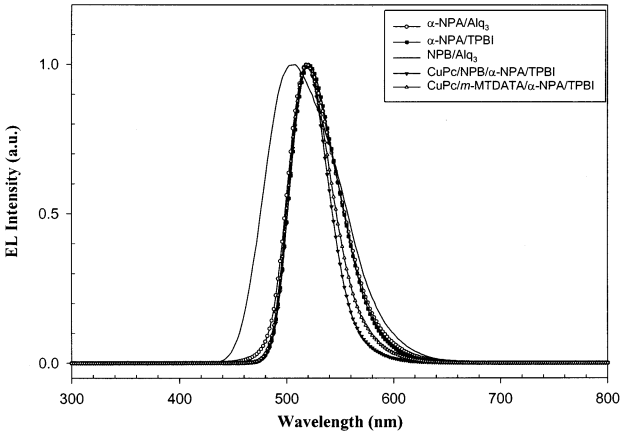

Figure 6. Electroluminescent spectra of devices **A** (α-NPA/Alq_3), **B** (α-NPA/TPBI), **C** (NPB/Alq_3), **G** (CuPc/NPB/α-NPA/TPBI), and **H** (CuPc/*m*-MTDATA/α-NPA/TPBI) at applied voltage 7 V.

bandwidths, 85[33] and 82 nm (Figure 6). The observations strongly indicate that the α-NPA instead of Alq_3 layer is responsible for the emission of the green light. These results are in contrast to a vast number of electroluminescent devices using arylamines as the hole-transport materials and Alq_3 as the electron-transport material.[1,3−5,34,35] In these devices, light generally emits from the Alq_3 layer due in part to the fact that hole mobility in the arylamine layer is faster than the electron migration in Alq_3 by a magnitude of a few orders and holes and electrons recombine in the Alq_3 layer.[36]

To further show that α-NPA is responsible for the emission in the device, a two-layer device **B** using α-NPA (40 nm) as the emitter and hole transporter and TPBI (50 nm) as the hole blocker and electron transporter was fabricated. The key properties of **B** are also listed in Table 2. As expected, the device emits green light from the α-NPA layer at 520 nm with a fwhm of 52 nm (Figure 6). Both devices **A** and **B** are very similar in bandwidth, wavelength, and thus the CIE values, strongly supporting the belief that the two devices emit light from the α-NPA layers. In view of the fact that devices **A** and **B** emit green light with wavelengths very near those based on Alq_3 as the emitter, a standard Alq_3 device **C**, consisting of the following layers: ITO/α-NPB-(40 nm)/Alq_3(50 nm) was built for close comparison using the same equipment for devices **A** and **B**. The EL spectrum of **C** is displayed in Figure 6, while the key properties of **C** are listed in Table 2. The results in Figure 6 and Table 2 clearly show that the emission bandwidths of devices **A** and **B** are much narrower than that of **C**.

By modification of the hole-transport layer, the emitting ability and efficiency of α-NPA can be further improved. In device **D**, a α-NPB layer (20 nm) was first deposited on ITO and then followed by α-NPA and TPBI layers. The maximum luminance and cd/A of this device were 38534 cd/m^2 and 7.28, respectively, improved by ca. 30% compared to those of device **B**. The use of *m*-MTDATA as the hole-injection layer brings further improvement in the performance of the devices. For device **E** with the following layer structure ITO/*m*-MTDATA(20 nm)/α-NPA(40 nm)/Alq_3(50 nm), the maximum brightness, external quantum efficiency, and cd/A are 43364 cd/m^2, 3.12%, and 11.92, while for device **F**, these values further increase to 65129 cd/m^2, 3.07%, and 12.05. The deposition of a thin buffer CuPc layer on ITO glass prior to the deposition of hole-injection material has been employed to enhance the hole-injection efficiency of a device.[4] We also use this technique in our present devices. Although the brightness and other properties of the devices do not improve as expected, the fwhm's are further reduced to <50 nm. As a result, the CIE of the devices with the presence of a thin CuPc layer were further improved and appeared at the region very close to that of the NTSC standard green ($x = 0.22$, $y = 0.71$) (Figure 5).[22] The EL spectra and properties are also shown in Figure 6 and Table 2, respectively.

Devices **I**−**L** and **M**−**P** were constructed to understand the electroluminescent and hole-transporting behavior of β-NPA and PPA, respectively. Key electroluminescent data extracted from the luminance and current density versus voltage characteristics are listed in Tables 3 and 4, while the CIE coordinates and the electroluminescent spectra of these devices are shown in Figures 5, 7, and 8. In the two-layer devices **I** and **M** consisting of the components β-NPA (or PPA)/Alq_3, the diaminoanthracene derivative acts as a hole transporter and a host emitter. Again, the light emits from the hole-transporting layer instead of the Alq_3 layer in these two devices The employment of *m*-MTDATA as a hole-

(33) The value is slightly different from that reported previously, see: Kido, J.; Iizumi, Y. *Appl. Phys. Lett.* **1998**, *73*, 2721.
(34) Wu, I. Y.; Lin, J. T.; Tao, Y. T.; Balasubramaniam, E.; Su, Y. Z.; Ko, C. W. *Chem. Mater.* **2001**, *13*, 2626.
(35) Thomas, K. R. J.; Lin, J. T.; Tao, Y. T.; Ko, C. W. *Chem. Mater.* **2002**, *14*, 1354.
(36) Hosokawa, C.; Tokailin, H.; Higashi, H.; Kusumoto, T. *Appl. Phys. Lett.* **1992**, *60*, 1220.

Table 4. Performance of PPA-Based OLEDs[a]

device[b]	turn-on voltage (V)	external quantum efficiency (%, V)	brightness (cd/m^2, V)	current efficiency (cd/A, V)	power efficiency (lm/W, V)	CIE (x, y)	λ_{max} (nm)	fwhm (nm)
M	2.7	1.92, 6.5 (1.84, 7.9)	31947, 12.0 (6668)	6.99, 6.5 (6.69)	4.71, 3.5 (2.67)	0.32, 0.59	522	79
N	4.0	2.91, 8.0 (2.55, 10.8)	40144, 15.0 (9282)	10.59, 8.0 (9.31)	5.05, 5.5 (2.70)	0.34, 0.59	518	85
O	4.4	2.93, 8.0 (2.55, 11.1)	42915, 15.5 (9198)	10.60, 8.0 (9.20)	5.54, 4.5 (2.60)	0.33, 0.59	518	85
P	4.0	2.05, 8.0 (1.95, 9.7)	36171, 14.0 (6907)	7.29, 8.0 (6.92)	3.04, 7.0 (2.25)	0.24, 0.65	518	52

[a] The data for external quantum efficiency, brightness, current efficiency, and power efficiency are the maximum values of the device, and those in the parentheses were taken at a current density of 100 mA/cm^2. [b] Device **M**, PPA(40 nm)/Alq_3(50 nm); **N**, *m*-MTDATA(20 nm)/PPA(40 nm)/Alq_3(50 nm); **O**, *m*-MTDATA(20 nm)/PPA(40 nm)/TPBI(50 nm); **P**, CuPc(10 nm)/*m*-MTDATA(20 nm)/PPA(40 nm)/Alq_3(50 nm).

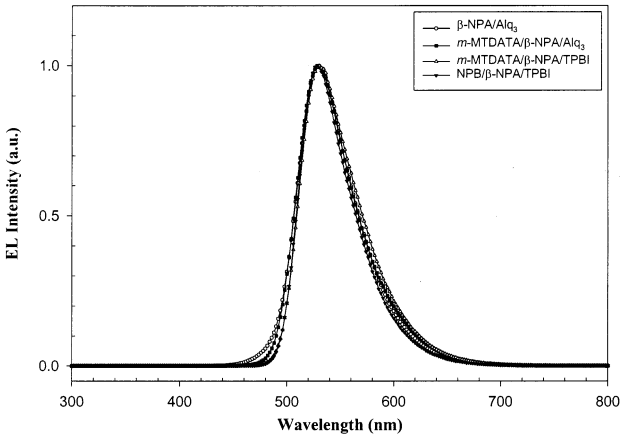

Figure 7. Electroluminescent spectra of devices **I** (β-NPA/Alq_3), **J** (*m*-MTDATA/β-NPA/Alq_3), **K** (*m*-MTDATA/β-NPA/TPBI), and **L** (NPB/β-NPA/TPBI) at applied voltage 7 V.

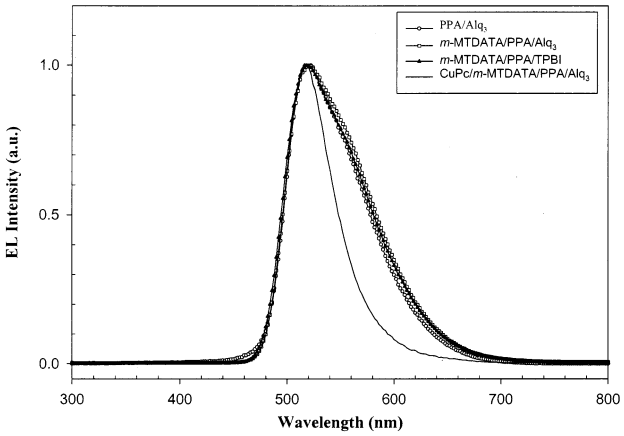

Figure 8. Electroluminescent spectra of devices **M** (PPA/Alq_3), **N** (*m*-MTDATA/PPA/Alq_3), **O** (*m*-MTDATA/PPA/TPBI), and **P** (CuPc/ *m*-MTDATA/PPA/Alq_3) at applied voltage 7 V.

injection layer and TPBI as the hole-blocking and electron-transporting layer (see devices **K** and **O** in Tables 3 and 4) greatly improve the external quantum efficiency, current efficiency, brightness, and power efficiency. For device **K**, the maximum current efficiency reaches 14.8 cd/A, the highest among the devices fabricated in the present paper. The wavelengths of the light emitted from β-NPA-based devices are slightly longer than those from the α-NPA- and PPA-based ones. To the best of our knowledge, the observed electroluminescent data of devices are among the best ones ever recorded for devices that emit green light directly from a fluorescent material used as host emitters.[14,16,23,26]

In conclusion, we have demonstrated that the diaminoanthracene derivatives are both green host emitters and hole-transport materials. Some of these materials exhibit excellent physical properties such as remarkable thermal stability and high melting and glass-transition points. The diaminoanthracene-derivatives-based electroluminescent devices emit green light at a wavelength of ca. 520 nm with extremely high brightness, current efficiency, narrow fwhm, and excellent CIE coordinates. Moreover, in contrast to most Alq_3-based green-emission devices, they give off light from the diaminoanthracene layer. The diaminoanthracene groups appear responsible for the highly emissive capability of these compounds.

Acknowledgment. We thank the Ministry of Education (Grant 89-FA04-AA) for the support of this research.

CM020414M